Smart Structures and Systems, *Vol. 29, No. 5 (2022) 677-691*
https://doi.org/10.12989/sss.2022.29.5.677

Metaheuristic-designed systems for simultaneous simulation of thermal loads of building

Chang Lin and Junsong Wang*

School of Architecture, South China University of Technology, 381 Wushan Road, Tianhe District, Guangzhou, Guangdong 510640, China

(*Received December 18, 2020, Revised November 13, 2021, Accepted February 10, 2022*)

Abstract. Water cycle algorithm (WCA) has been a very effective optimization technique for complex engineering problems. This study employs the WCA for simultaneous prediction of heating load (L_H) and cooling load (L_C) in residential buildings. This algorithm is responsible for optimally tuning a neural network (NN). Utilizing 614 records, the behavior of the L_H and L_C is explored and the captured knowledge is then used to predict for 154 unanalyzed building conditions. Since the WCA is a population-based algorithm, different numbers of the searching agents were tested to find the most optimum configuration. It was observed that the best solution is discovered by 500 agents. A comparison with five newly-developed benchmark optimizers, namely equilibrium optimizer (EO), multi-tracker optimization algorithm (MTOA), slime mould algorithm (SMA), multi-verse optimizer (MVO), and electromagnetic field optimization (EFO) revealed that the WCANN predicts the desired parameters with considerably larger accuracy. Obtained root mean square errors (1.4866, 2.1296, 2.8279, 2.5727, 2.5337, and 2.3029 for the L_H and 2.1767, 2.6459, 3.1821, 2.9732, 2.9616, and 2.6890 for the L_C) indicated that the most reliable prediction was presented by the proposed model. The EFONN, however, provided a more time-effective solution. Lastly, an explicit predictive formula was elicited from the WCANN.

Keywords: cooling load; energy performance; heating load; neural computing; water cycle algorithm

1. Introduction

Today, energy-efficiency analysis is a very crucial field of study, due to its effect on different sectors (Chung *et al*. 2006, Palm and Thollander 2010, Ahmadi-Karvigh *et al*. 2018). For instance, building construction and related tasks are responsible for up to 36% of global final energy consumption, and also, around 39% CO_2 emission corresponding to energy (IEA 2019).

Environmental objectives like reducing greenhouse gas emissions (Vine 2003), economical issues like optimizing the energy consumption (Dunlop 2019), and satisfying living standards in today smart cities (Silva *et al*. 2018) are only a few reasons for utilizing state-of-the-art equipment like heating, ventilating, and air conditioning (HVAC) system (McQuiston *et al*. 1982) in modern buildings. But selecting the appropriate approach for tuning and analyzing such systems is of great importance. In Hong Kong, for example, air conditioning systems are responsible for taking around one-third of electricity used in the buildings (EMSD 2019).

Many recent developments have occurred after introducing sophisticated technologies like digital imagery (Xu *et al*. 2021), soft computing (Zhou *et al*. 2021b), satellite monitoring (Zhang *et al*. 2019), remote sensing (Li and Zhang 2008) that served for simulations in various fields of study (Schwalm *et al*. 2013, Gor and Kurt 2016, Feng *et al*. 2021, Li *et al*. 2021b, Zhang *et al*. 2021). Soft computing are among the most popular techniques, due to their advantages in heavy calculations. They have powerfully handled engineering simulations like power of generators (Kurt and Gör 2014, Çelik *et al*. 2017, Çelik and Gör 2019), geohazard assessments (Nguyen *et al*. 2019), energy efficiency (Ekici and Aksoy 2011), gas emissions (Ghiasi *et al*. 2016), etc.

Energy efficiency-related issues have been successfully modeled using soft computing tools like artificial neural network (ANN) (Alam *et al*. 2016, Li *et al*. 2021a) and regression-based models (Reddy and Kumar 2019). Macas *et al*. (2016) developed an ANN-based predictor for modeling the parameters, namely total heating energy consumption, internal air temperature, and aggregated thermal discomfort for an office building. Moreover, scholars like Homod *et al*. (2020) and Yaïci and Entchev (2016) have considered the use of adaptive neuro-fuzzy inference system (ANFIS) for thermal energy and HVAC analysis. Nilashi *et al*. (2017) used this model with a noise removal point of view. The low values of error confirmed the sufficient accuracy of their results. Support vector machine (SVM) is another robust machine learning model that has been highly regarded for energy-efficiency predictions (Li *et al*. 2009a, Koschwitz *et al*. 2018).

Seyedzadeh *et al*. (2019) investigated the applicability of several machine learning models for predicting the L_H and L_C of buildings with various usages including restaurant, hotel, office, etc. Their research showed the high

*Corresponding author, Ph.D.,
E-mail: arwjs@mail.scut.edu.cn
[a] Ph.D., E-mail: linlinc@aliyun.com

ISSN: 1738-1584 (Print), 1738-1991 (Online)

capacity of random forest (RF), gradient boosted regression trees, ANN, SVM, and gaussian process (GP) for this purpose. Roy *et al*. (2018) employed extreme learning machine (ELM) and multivariate adaptive regression splines (MARS) for energy modeling. They developed an ensemble using these two approaches wherein the ELM is applied to the parameters outlined by the MARS. The RMSEs of 0.0525 vs. 0.2573 and 0.1002 for the L_H and 0.1952 vs. 0.3170 and 0.1950 for the L_C dataset showed that the simultaneous use of both models results in a more accurate prediction of the mentioned parameters. Moradzadeh *et al*. (2020) proved the competency of support vector regression (SVR) and multilayer perceptron (MLP) for the same simulation. Moreover, an innovative ensemble of the SVR and ANN was proposed by Chou and Bui (2014) as an efficient predictive tool for analyzing the thermal loads. In a comparative work, Kumar *et al*. (2018) showed the superiority of online sequential ELM over classical approaches like ANN, SVM, and RF. Further comparisons between various data mining techniques are sufficiently available in the earlier literature (Li *et al*. 2009b, Zhao and Liu 2018).

Apart from machine learning models, many recent studies have argued the efficiency of metaheuristic algorithms in various engineering domains (Nehdi and Greenough 2007, Hakim and Razak 2014, Shariati *et al*. 2020, Ye *et al*. 2020) (e.g., building energy consumption (Chou and Ngo 2016, Tran *et al*. 2020), operating schedule of sources (Ikeda and Ooka 2015), fuel consumption (Zeynali *et al*. 2020), HVAC calibration (Martin *et al*. 2019), renewable energy system (Das *et al*. 2019), etc.).

These methods have promisingly served for predicting the thermal loads in various types of buildings. Seyedzadeh *et al*. (2020) used a multi-objective optimization method for tuning machine learning tools in estimating the L_H and L_C. Bui *et al*. (2020) found the combination of ANN with electromagnetism-based firefly algorithm a suitable approach for analyzing the loads of energy-efficient buildings. Le *et al*. (2019b) presented a combination of particle swarm optimization (PSO) and XGBoost for the same objective. With respective RMSEs of 1.124, 1.779, 1.632, 1.598, 1.776, and 1.651, the proposed model outperformed intelligent models including classification and regression trees, GP, RF, SVM, and classical XGBoost. Wu *et al*. (2020) evaluated the efficiency of backtracking search algorithm (BSA) and vortex search algorithms (VSA) in combination with ANN for predicting the L_H. They showed that the model developed by the VSA is suitable for sensitive estimations, while the BSA provides a faster prediction and is more time-effective. Similarly for the L_C modeling, Zhou *et al*. (2020b) coupled the ANN with teaching–learning-based optimization. They introduced the proposed model as an accurate approach for the early assessment of L_C, due to its better performance compared to the benchmarks of league championship algorithm and cuckoo optimization algorithm (R^2s of 0.9207 vs. 0.9120 and 0.9068). In a comparitive effort, the feasibility of four well-known optimizers, namely artificial bee colony (ABC) optimization, imperialist competitive algorithm, PSO, and genetic algorithm for simulating the L_H was investigated by Le *et al*. (2019a). Comparison of the results revealed the largest accuracy for the latest optimizer for constructing the ANN (RMSEs of 1.625 vs. 1.878, 1.982, and 1.932).

Generally speaking, the use of metaheuristic algorithms along with conventional predictors results in curing shortcomings like local minimum and dimension dangers (Mehrabi *et al*. 2020). Further applications of other metaheuristic algorithms like stochastic fractal search (SFS) (Moayedi and Mosavi 2021a), shuffled complex evolution (SCE) (Zheng *et al*. 2020) for thermal load modeling can be found in previous literature (Al-Shammari *et al*. 2016, Moayedi *et al*. 2020). Following the promising usages of these techniques in dealing with the non-linear prediction of thermal loads, this study pursues a comprehensive evaluation of several recently-developed optimizers applied to an ANN for simulating the L_H and L_C. The main suggested algorithm is water cycle algorithm (WCA) and its performance is compared with equilibrium optimizer (EO), multi-tracker optimization algorithm (MTOA), slime mould algorithm (SMA), multi-verse optimizer (MVO), and electromagnetic field optimization (EFO). The optimal configuration of each neural-hybrid is discovered and the prediction results, as well as the optimization efficiency, are discussed to introduce an efficient model for the mentioned objective. Further, comparing the findings of the present study with previous similar works is presented at the end. It can reflect the improvements done and discover the advantages of the metaheuristic strategies.

2. Methodology and data

2.1 Dataset

Collected by Tsanas and Xifara (2012), a valuable dataset was provided by executing a vast computer modeling in the Ecotect environment (Roberts and Marsh 2001). The assumptions and the results of a total of 768 stages were recorded to create the mentioned dataset wherein the L_H and L_C are the functions of eight factors, namely relative compactness (C_R), surface area (S_A), wall area (S_W), roof area (S_R), overall height (H_T), orientation (O), glazing area (S_G), and glazing area distribution (DS_G). Accordingly, for this study, the L_H and L_C are the target parameters, while the C_R, S_A, S_W, S_R, H_T, O, S_G, and DS_G play the role of the input parameters. The used dataset is available on:
http://archive.ics.uci.edu/ml/datasets/Energy+efficiency.

Famously, each input factor, depending on its definition, has a specific effect on the L_H and L_C parameters. For instance, relative compactness expresses the portion of the surface area relative to the corresponding volume (Ouarghi and Krarti 2006) and glazing area accounts for the glazing measured with the rough opening (e.g., frame and sash glazing) (Zhou *et al*. 2020a). For more details regarding these influential parameters, previous literature like (Tsanas and Xifara 2012, Huang *et al*. 2014) may be read.

Fig. 1 shows the patterns of the input and target parameters. As is seen, all inputs follow a regular pattern in the present sequence except the S_G which rises from 0.0 to 0.4 in three steps.

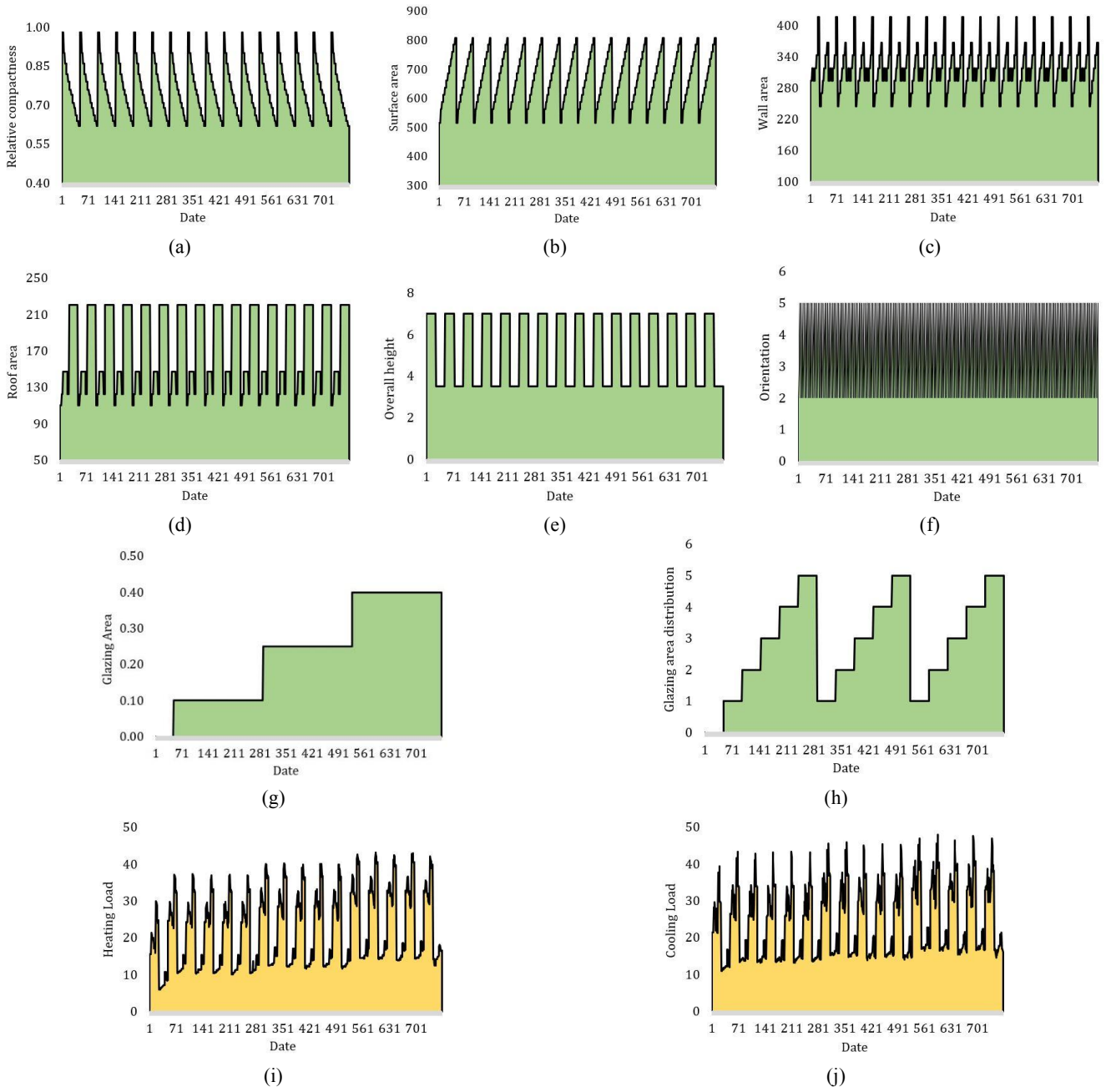

Fig. 1 The variations in the LH, LC, and input factors

2.2 Statistical analysis

Moreover, Table 1 gives the statistical indicators (i.e., average, standard error, sample variance, minimum, and maximum values) along with the input-target correlations. According to this table, the most correlated parameter is H_T with the coefficients of determination (R^2s) of 0.7911 and 0.8024 with the L_H and L_C, respectively. Furthermore, the R^2 of 0.9523 says that target parameters are directly proportional to each other.

In studies by Zheng *et al*. (2020) and Wu *et al*. (2020) the importance of these input parameters was investigated on the prediction of L_C and L_H, respectively. They performed a permutation-based importance assessment using a random forest model. It was shown that S_G and C_R play the most important roles for this task. Also, the smallest contribution was observed for the SW, HT, and O.

Famously, apart from training the models, a developed model needs a number of intact data (i.e., unanalyzed records) to assess its generalization ability. In this relation, 80% of the whole (i.e., 614 records) are randomly used to train the suggested hybrids and the remaining 154 records form the testing dataset.

2.3 Methodology

Fig. 2 exhibits the methodology considered for fulfilling the purpose of this research. The data provision was followed by statistical analysis and division to training and testing sets. After that, the models are developed by

Table 1 Descriptive statistics of the LH, LC, and input factors

Parameter	Descriptive indicator						
	Mean	Standard error	Sample variance	Minimum	Maximum	R^2 with L_H	R^2 with L_C
C_R	0.76	0.00	0.01	0.62	0.98	0.3872	0.4024
S_A	671.71	3.18	7759.16	514.50	808.50	0.4331	0.4529
S_W	318.50	1.57	1903.27	245.00	416.50	0.2076	0.1824
S_R	176.60	1.63	2039.96	110.25	220.50	0.7427	0.7440
H_T	5.25	0.06	3.07	3.50	7.00	0.7911	0.8024
O	3.50	0.04	1.25	2.00	5.00	7E-06	0.0002
S_G	0.23	0.00	0.02	0.00	0.40	0.0728	0.0431
DS_G	2.81	0.06	2.41	0.00	5.00	0.0076	0.0026
L_H	22.31	0.36	101.81	6.01	43.10	1.0000	0.9523
L_C	24.59	0.34	90.50	10.90	48.03	0.9523	1.0000

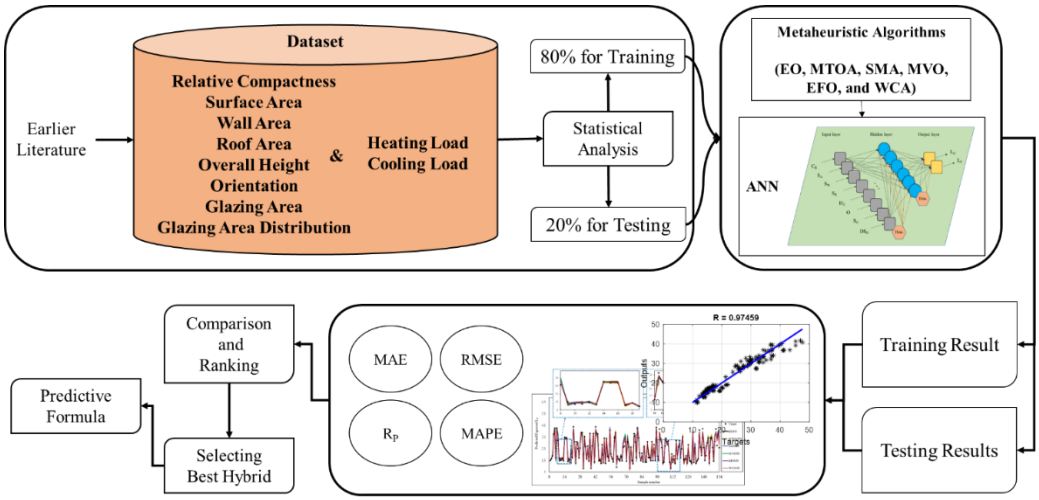

Fig. 2 The schematic methodology of the study

2.3.1 The ANN

Based on the mechanism of a biological neural network, the ANN (Anderson and McNeill 1992) was designed as a non-linear processing system. Up to now, different types of this tool have attracted growing attention for complex engineering simulations like shock waves after dam break (Seyedashraf *et al*. 2018), natural gas consumption (Qiao *et al*. 2020), landslide susceptibility (Moayedi *et al*. 2019), wind speed (Zhang *et al*. 2020), etc.

An MLP (Hornik *et al*. 1989, Pinkus 1999) is a robust type of the ANNs which, as is implied by its name, is composed of some layers with a number of processors called node. Fig. 3 gives an illustration of the MLP that predicts the L_H and L_C in this study. As is seen, these parameters are calculated by the output nodes. The weights that link the hidden and output layers, as well as two bias terms, are used for this calculation. The same strategy is implemented in the nodes of the former layer. Assuming $K = (K_1, K_2, ..., K_Z)$ as a typical input vector, f as the activation function, and $W = (W_1, W_2, ..., W_Z)$ and $B = (B)$ as the weight and bias vectors, respectively, the below equation describes the computations of a node.

$$Output = f(W_1 \times K_1 + W_2 \times K_2 + \cdots W_Z \times K_Z + B) \quad (1)$$

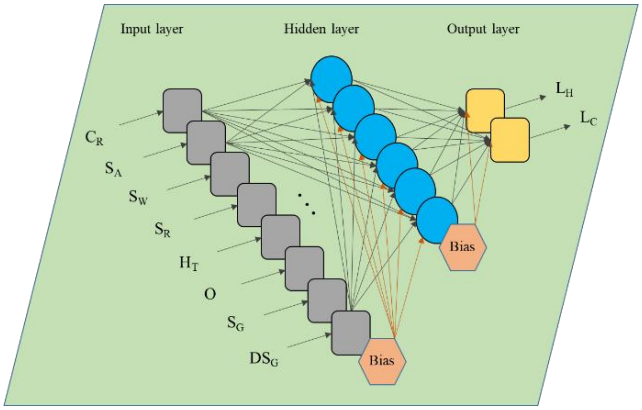

Fig. 3 A three-layer MLP

A so-called scheme "back-propagation" (Hecht-Nielsen 1992) is executed in a classical MLP to minimize the error. In this scheme, the error of each iteration is calculated and the algorithm propagates backward to re-tune the computational parameters. In this work, this scheme is replaced with several metaheuristic strategies to train the MLP.

2.3.2 The WCA strategy

Mimicking the typical water cycle, the WCA was introduced by Eskandar *et al*. (2012). This algorithm has acted as a highly capable optimizer in dealing with diverse problems (Nasir *et al*. 2020). For example, Foong *et al*. (2020) used a modified WCA for optimizing the ANN applied to predict soil shear strength.

The algorithm starts with creating the random population. Three components of the population are streams, rivers, and the sea. Once the raindrops reach the earth, the best-fitted ones form the sea, those in the next class of fitness form the rivers, and the rest form the streams. In other words, the fitness is the criterion for classifying the components. Given S_{total} as the size of the whole population and S_{RS} as the number of rivers plus the sea (i.e., $S_{RS} = S_{rivers} + 1$), the number of streams is obtained as follows

$$S_{streams} = S_{total} - S_{RS} \tag{2}$$

Due to the differences in the flow magnitudes, each stream brings a different amount of water to the sea or rive. Let g be the evaluative function of the WCA, then, the number of streams that bring the water to particular rivers is given as follows

$$NS_j = round\left\{\left|\frac{g(River_j)}{\sum_{i=1}^{S_{RS}} g(River_i)}\right| \times S_{streams}\right\}, \quad j = 1, 2, \ldots, S_{RS} \tag{3}$$

The streams chose a random distance to flow into the rivers through some linking paths. Given *cd* as the current distance between them, Eq. (4) produces a randomly distributed distance for this process.

$$X \in (0, M \times cd) \quad M > 1 \tag{4}$$

where M signifies a criterion for determining the flow procedure. More clearly, M > *1* indicates that the streams can choose diverse directions to join the rivers. The same concept can be considered for the rivers joining the sea. In this relation, Eqs. (5) and (6) define the new positions of the streams and rivers, respectively.

$$X_{stream}^{new} = X_{stream}^{old} + rand \times M \times (X_{river}^{old} - X_{stream}^{old}) \tag{5}$$

$$X_{river}^{new} = X_{river}^{old} + rand \times M \times (X_{sea} - X_{river}^{old}) \tag{6}$$

where X_{River}^{old} and X_{stream}^{old} stand for the former positions of the corresponding components. Likewise, X_{Sea} represents the position of the sea. Once the new positions of the streams provide better-fitted solutions compared to the current river, they exchange positions. The same goes for the new rivers and the sea.

Repeating the raining process is an idea that prevents problems like local minima. Eq. (7) defines a criterion for checking the quality of the discovered solution (Luo *et al*. 2016).

$$\text{If} \quad |X_{sea} - X_{river}| < \varepsilon \tag{7}$$

2.3.3 Benchmark strategies

It was earlier mentioned that the performance of the WCA is assessed relative to five other metaheuristic algorithms including the EO, MTOA, SMA, MVO, and EFO. In other words, these algorithms play the role of benchmarks for the WCA. Similar to the WCA, they represent population-based algorithms that aim to optimally find solutions to the problem of L_H and L_C prediction. As a matter of fact, each metaheuristic algorithm simulates a specific strategy to perform the optimization. For example,

Table 2 Description of the benchmark metaheuristic algorithms

Algorithm	Developer(s)	Year	Inspiration	Strategy	Examples of uses
EO	Faramarzi *et al*. (2020)	2020	Equilibrium state	An equilibrium pool is created that contains four agents with the largest fitness plus one agent with their average fitness. By taking equilibrium rules, the concentration of the agents is updated.	(Abdel-Basset *et al*. 2020, Yıldız *et al*. 2020)
MTOA	Zakeri *et al*. (2017)	2017	Local and global tracking	First, global trackers find a global optimal point, then, local trackers search a certain radius around them to discover local optimal points.	(Khosravi *et al*. 2020, Liang *et al*. 2020)
SMA	Li *et al*. (2020)	2020	Dynamic nutritional behavior of slime mould	The slime mould searches an interconnected venous network having multiple food blocks and finds the optimal path toward the largest concentration of nutrients.	(Brabazon and McGarraghy 2020, Li *et al*. 2020)
MVO	Mirjalili *et al*. (2016)	2016	Multiverse theory	Utilizing three cosmological components, namely worm hole, black hole, and white hole, the objects are transferred from the universe with high inflation to those with low inflation to improve the average inflation of the entire cosmoses.	(Jangir *et al*. 2017, Fathy and Rezk 2018)
EFO	Abedinpourshotorban *et al*. (2016)	2016	Electromagnetic rules	Electromagnetic particles are classified in three fields, namely positive field, negative field, and neutral field. By taking electromagnetic rules, new particles are generated and the good ones replace former particles in the population.	(Talebi and Dehkordi 2018, Song *et al*. 2019)

in the case of this study, the optimal sea in the WCA is identified as the optimized parameters (i.e., the biases and weights) for constructing the ANN.

Table 2 describes the EO, MTOA, SMA, MVO, and EFO. In these methods, a number of search agents are randomly generated where each of which has a fitness value. The fitnesses are increased toward the ideal as the iterations go forward. Once a stopping criterion is satisfied, the optimization is terminated and the latest solution is saved.

2.4 Accuracy indicators

For the prediction of both L_C and L_H, four popular indicators, namely mean absolute error (MAE), root mean square error (RMSE), mean absolute percentage error (MAPE), and Pearson correlation coefficient (R_P) are used to assess the accuracy in different ways. Let Q signify the number of samples and $L_{i_{predicted}}$ and $L_{i_{expected}}$ be the predicted and expected loads, respectively, the MAE, RMSE, MAPE, and R_P are defined based on Eqs. (8) to (11).

$$MAE = \frac{1}{Q}\sum_{i=1}^{Q}|L_{i_{expected}} - L_{i_{predicted}}| \quad (8)$$

$$RMSE = \sqrt{\frac{1}{Q}\sum_{i=1}^{Q}[(L_{i_{expected}} - L_{i_{predicted}})]^2} \quad (9)$$

$$MAPE = \frac{1}{Q}\sum_{i=1}^{Q}\left|\frac{L_{i_{expected}} - L_{i_{predicted}}}{L_{i_{expected}}}\right| \times 100 \quad (10)$$

$$R_P = \frac{\sum_{i=1}^{Q}(L_{i_{predicted}} - \overline{L}_{predicted})(L_{i_{expected}} - \overline{L}_{expected})}{\sqrt{\sum_{i=1}^{Q}(L_{i_{predicted}} - \overline{L}_{predicted})^2}\sqrt{\sum_{i=1}^{Q}(L_{i_{expected}} - \overline{L}_{expected})^2}} \quad (11)$$

3. Results and discussion

This paper presents an efficient combination of neural network and water cycle algorithm for simultaneously predicting the L_H and L_C. To evaluate the potential of the WCA algorithm, several recent metaheuristic algorithms are also employed. These algorithms are responsible for tuning the ANN through their specific strategies. During this iterative proceeding, a huge number of solutions are tried and the best one is eventually used.

Fig. 4 shows the optimization process. The ANN used in this study, as shown in Fig. 3, contains 8 input neurons, 6 hidden neurons, and 2 output neurons. The equation of this raw ANN is initially received by the metaheuristic techniques. This equation is accordingly formed to contribute the inputs to the L_H and L_C. The prediction task is performed by tuning the weights and biases of this relationship. The prediction error is calculated by comparing the actual targets and predicted output. Utilizing an objective function (OF, which is the RMSE here), the algorithms minimize the error of prediction for the training data. This error is defined as the averaged RMSE of the L_H and L_C in each iteration. After executing the appropriate number of iterations, the ANN is re-constructed to predict the L_H and L_C. This strategy is repeated until the maximum number of iterations is reached. Note that, the whole process was implemented in Matlab v. 2017b. The findings of this process are presented in the following section.

3.1 Optimization and training

Fig. 5 shows the error minimization proceeding of the implemented models. Due to the optimization behavior of the algorithms, the EFO was implemented with 30000 iterations, while 1000 iterations were considered for other algorithms. This is why the figure has a secondary horizontal axis for the EFO iterations. The population size (N_{pop}) of each model was designated after a trial and error process. In this regard, the EO, MTOA, SMA, and MVO attained their best performance with N_{pop} = 400, while this value for the EFO and WCA was 25 and 500, respectively. As the magnified section of Fig. 5 illustrates, the OF of the WCANN is below those of other models. The average RMSEs obtained for the EONN, MTOANN, SMANN, MVONN, EFONN, and WCANN were 2.2205, 2.7906, 2.5687, 2.5988, 2.3500, and 1.8137, respectively.

Analyzing the training results showed that the ANNs created by all algorithms can predict both L_H and L_C with high consistency with expected values. The obtained accuracy indicators are presented in the respective order for the EONN, MTOANN, SMANN, MVONN, EFONN, and WCANN in the following. The RMSEs were 1.9188, 2.6076, 2.3268, 2.3512, 2.1240, and 1.4509 for the L_H, and 2.5221, 2.9736, 2.8106, 2.8463, 2.5760, and 2.1764 for the

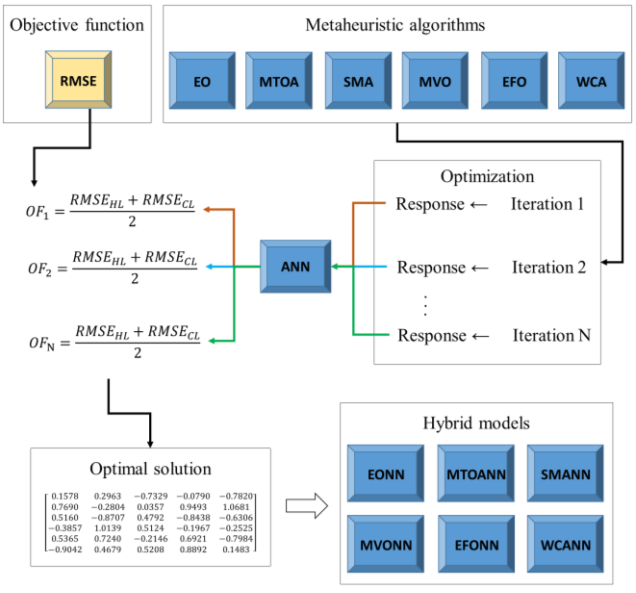

Fig. 4 Optimizing the ANN using metaheuristic algorithms

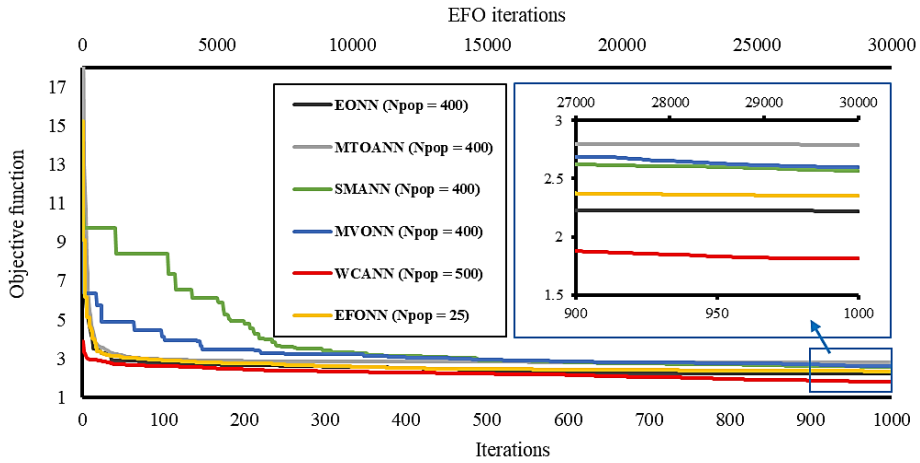

Fig. 5 The convergence proceeding of the used optimizers

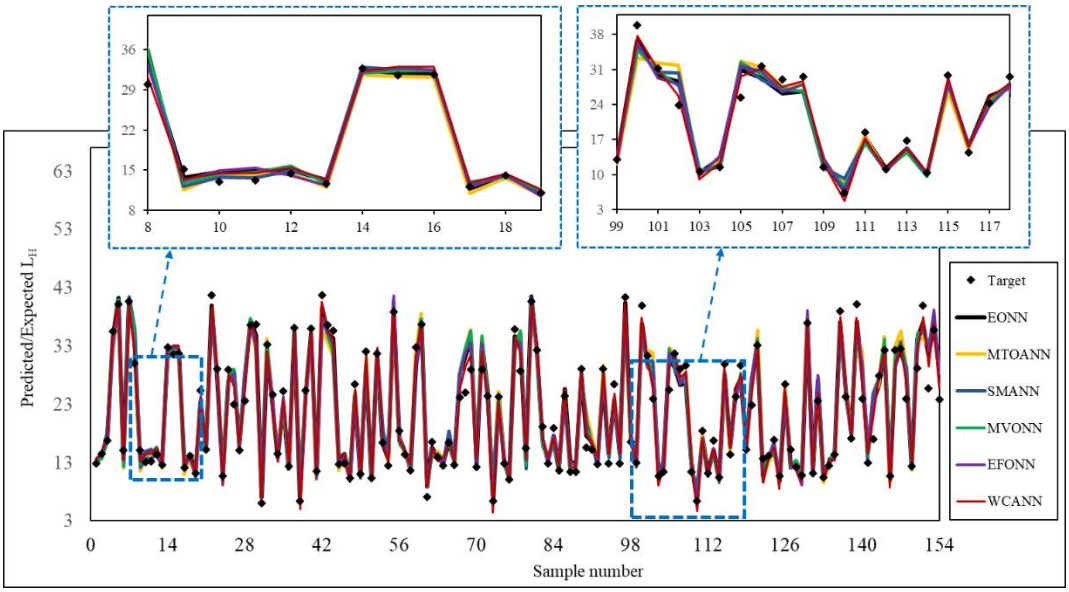

(a) L_H

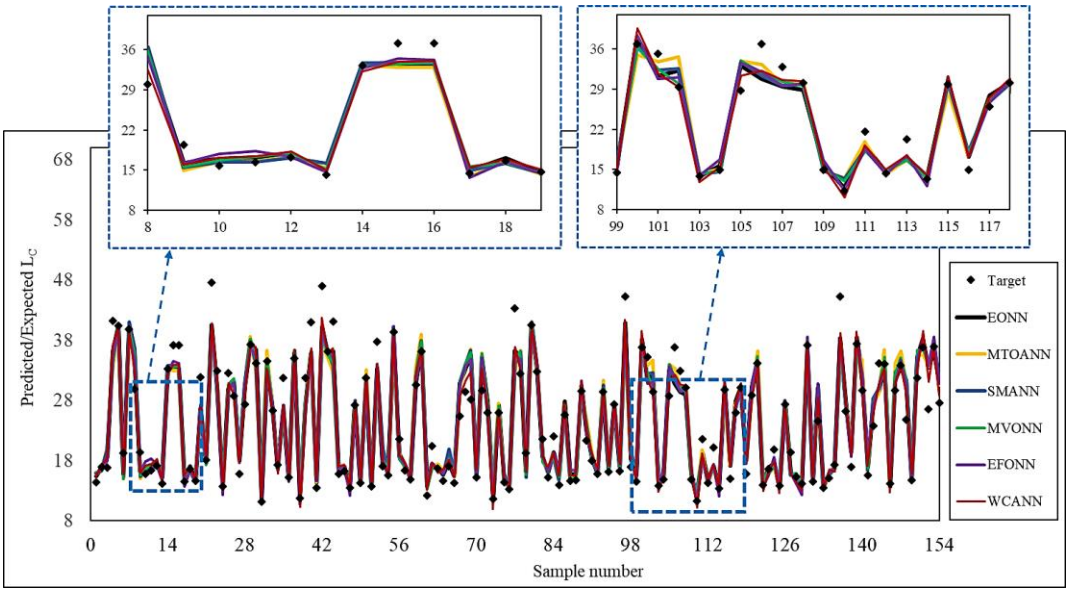

(b) L_C

Fig. 6 Graphical comparison between the expected values and the patterns predicted by the used models

L_C. These values, plus the MAEs of 1.3689, 1.8564, 1.6026, 1.6368, 1.5268, and 1.1333 for the L_H, and 1.7602, 2.0764, 1.9074, 1.9435, 1.8229, and 1.6625 for the L_C indicate a high-quality training for all the used hybrids. Moreover, the correlations indicator, i.e., the R_Ps of 0.9818, 0.9661, 0.9731, 0.9725, 0.9777, and 0.9896 for the L_H, and 0.9639, 0.9495, 0.9550, 0.9538, 0.9623, and 0.9734 for the L_C, indicated a very good agreement between the $L_{Predicted}$s and $L_{Expected}$s for both loads. The goodness of the results can be also demonstrated by low relative errors, i.e., the MAPEs of 6.2943, 8.6070, 7.5390, 7.5717, 7.0993, and 5.9030% for the L_H, and 7.0153, 8.2796, 7.8220, 7.8376, 7.4055, and 6.9193% for the L_C.

3.2 Prediction of the L_H and L_C

It was stated that all models could non-linearly capture a reliable perception of the dependence of the L_C and L_H on the C_R, S_A, S_W, S_R, H_T, O, S_G, and DS_G. For this process, the model used 614 samples. The generalizability of the captured patterns was evaluated by predicting the L_C and L_H for the second group of data, i.e., 154 testing samples. These records represent new building conditions for the models.

Figs. 6(a) and (b) give a graphical comparison between the predicted and expected values of L_H and L_C, respectively. According to these charts, all algorithms have correctly forecasted the behavior of both L_H and L_C. The RMSEs of 2.1296, 2.8279, 2.5727, 2.5337, 2.3029, and 1.4866, as well as the MAEs of 1.5234, 2.0080, 1.7630, 1.7976, 1.7284, and 1.1868 for the L_H, and the RMSEs of 2.6459, 3.1821, 2.9732, 2.9616, 2.6890, and 2.1767, as well as the MAEs of 1.8360, 2.1903, 2.0303, 2.0499, 1.9353, and 1.6469 for the L_C, indicates that both target parameters have been predicted with a high level of accuracy. Besides, the obtained MAPEs were 7.3066, 9.8225, 8.6652, 8.6394, 8.3812, and 6.6476 for the L_H, and 7.1106, 8.4742, 8.1296, 8.1691, 7.7458, and 6.9091 for the L_C that demonstrate a tolerable level of relative error for both predictions.

Moreover, Figs. 7 and 8 show the correlation between the predicted and expected values of L_H and L_C, respectively. At a glance, the products of all models are in excellent agreement (i.e., $R_P > 0.94$) with the expected L_Hs and L_Cs. The calculated R_Ps were 0.9772, 0.9596, 0.9667, 0.9680, 0.9731, and 0.9888 for the L_H, and 0.9616, 0.9436, 0.9511, 0.9515, 0.9602, and 0.9745 for the L_C.

In the L_H dataset, the lowest value is 6.0500 that is predicted to be 7.1278, 8.8575, 8.9185, 7.1323, 7.5789, and 5.8763, and the highest value is 41.7300 that is predicted to be 39.8879, 38.5303, 39.2090, 38.7216, 38.5241, and 39.7821. As for the L_C dataset, the lowest value is 11.1900 that is predicted to be 11.5755, 13.2845, 13.1070, 12.7263, 10.7447, and 9.9550, and the highest value is 47.5900 that is predicted to be 40.8158, 40.6395, 41.0489, 40.8048, 40.2522, and 41.7002.

3.3 Efficiency comparison

In the previous explanations, it was derived that all six algorithms can develop potential neural relationships to predict the L_H and L_C in the same network. But due to the main objective of the study (i.e., to assess the capability of the WCA), this section is concerned with the efficiency assessment of the employed models.

All accuracy indicators presented in the previous sections are given in Table 3. It also contains the same number of scores to compare the accuracy of the hybrids. These scores are assigned to each accuracy indicator (from 1 to 6) so that the better the prediction is, the larger the given score is. In the case of error indicators (i.e., RMSE,

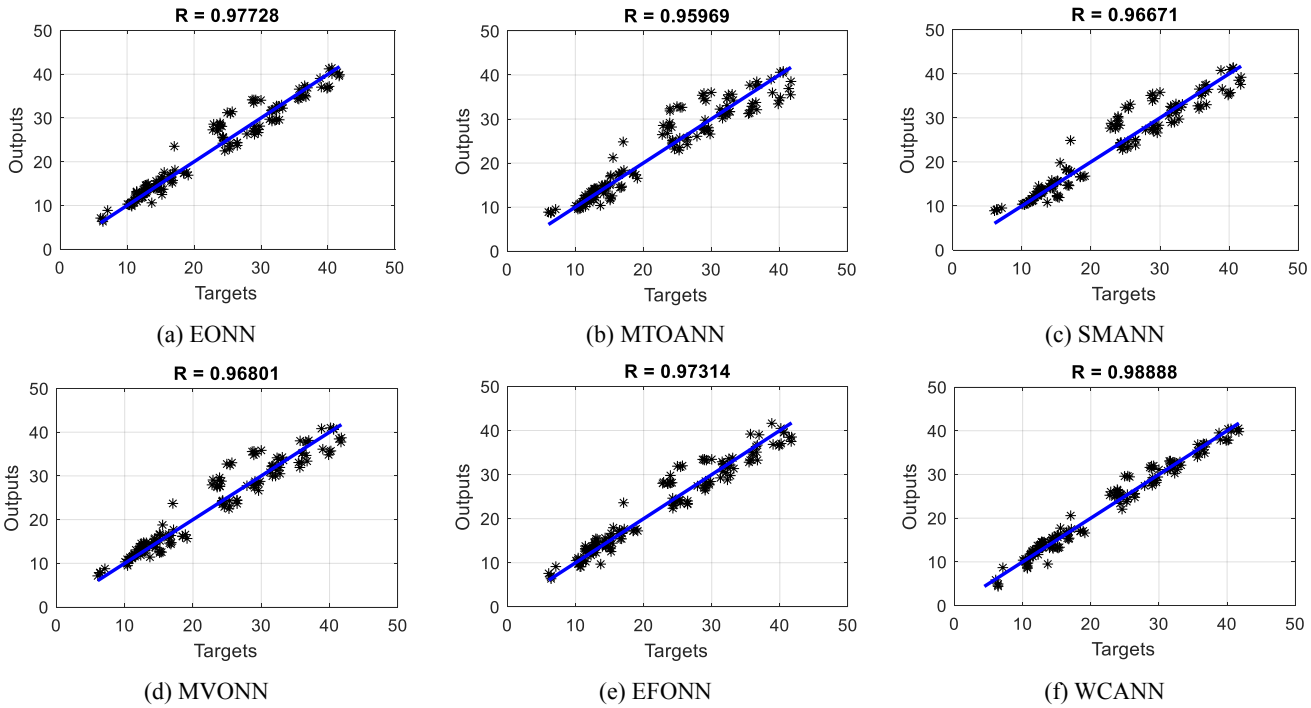

(a) EONN (b) MTOANN (c) SMANN

(d) MVONN (e) EFONN (f) WCANN

Fig. 7 The LH-testing results

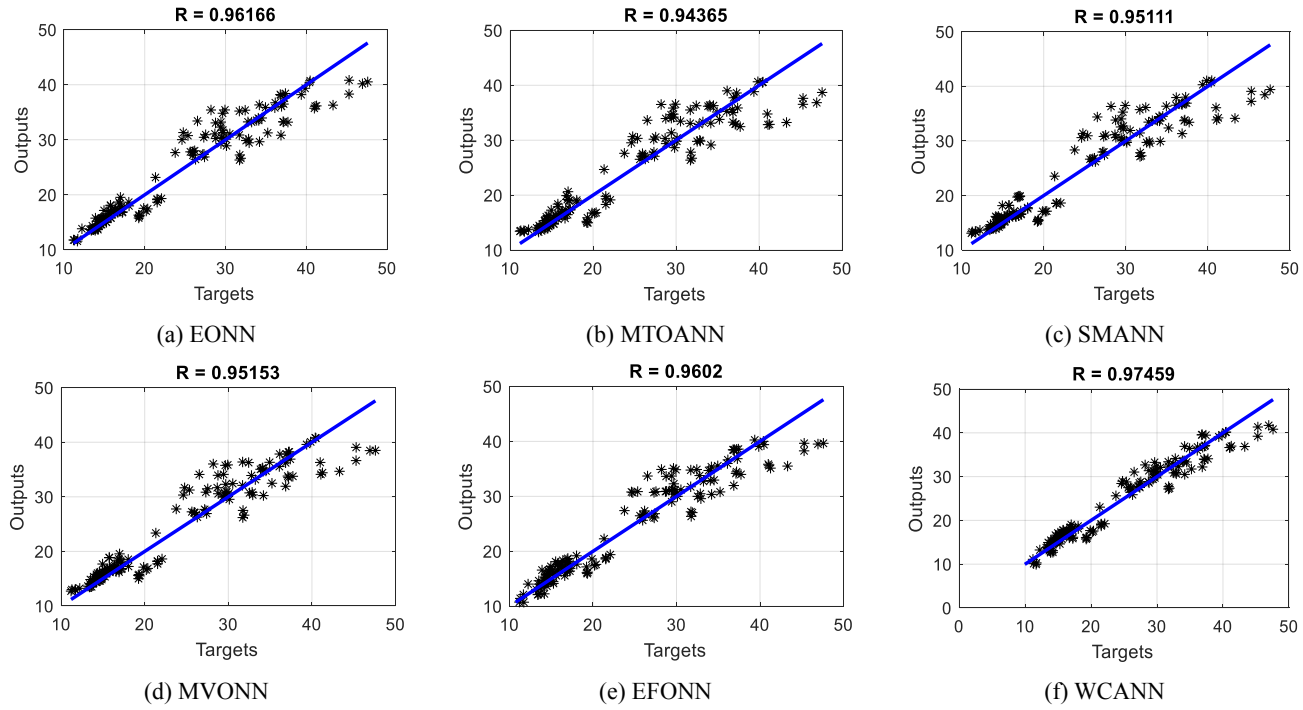

(a) EONN (b) MTOANN (c) SMANN

(d) MVONN (e) EFONN (f) WCANN

Fig. 8 The LC-testing results

Table 3 Ranking comparison of the used models

Accuracy criterion	Models	Data															
		Training								Testing							
		L_H				L_C				L_H				L_C			
		MAE	RMSE	R_p	MAPE	MAE	RMSE	R_p	MAPE	MAE	RMSE	R_p	MAPE	MAE	RMSE	R_p	MAPE
Indicator	EONN	1.3689	1.9188	0.9818	6.2943	1.7602	2.5221	0.9639	7.0153	1.5234	2.1296	0.9772	7.3066	1.8360	2.6459	0.9616	7.1106
	MTOANN	1.8564	2.6076	0.9661	8.6070	2.0764	2.9736	0.9495	8.2796	2.0080	2.8279	0.9596	9.8225	2.1903	3.1821	0.9436	8.4742
	SMANN	1.6026	2.3268	0.9731	7.5390	1.9074	2.8106	0.9550	7.8220	1.7630	2.5727	0.9667	8.6652	2.0303	2.9732	0.9511	8.1296
	MVONN	1.6368	2.3512	0.9725	7.5717	1.9435	2.8463	0.9538	7.8376	1.7976	2.5337	0.9680	8.6394	2.0499	2.9616	0.9515	8.1691
	EFONN	1.5268	2.1240	0.9777	7.0993	1.8229	2.5760	0.9623	7.4055	1.7284	2.3029	0.9731	8.3812	1.9353	2.6890	0.9602	7.7458
	WCANN	1.1333	1.4509	0.9896	5.9030	1.6625	2.1764	0.9734	6.9193	1.1868	1.4866	0.9888	6.6476	1.6469	2.1767	0.9745	6.9091
Score	EONN	5	5	5	5	5	5	5	5	5	5	5	5	5	5	5	5
	MTOANN	1	1	1	1	1	1	1	1	1	1	1	1	1	1	1	1
	SMANN	3	3	3	3	3	3	3	3	3	2	2	2	3	2	2	3
	MVONN	2	2	2	2	2	2	2	2	2	3	3	3	2	3	3	2
	EFONN	4	4	4	4	4	4	4	4	4	4	4	4	4	4	4	4
	WCANN	6	6	6	6	6	6	6	6	6	6	6	6	6	6	6	6

MAE, and MAPE), they are adversely proportional to the score values, while it is the opposite for the R_P.

According to the obtained scores, the ANNs trained by the WCA, EO, EFO achieved the scores of 6, 5, and 4 in terms of all accuracy indicators for both L_H and L_C, and consequently, they are ranked as the first, second, and third-accurate models in the present study, respectively. Besides, acquiring a score of 1 all over the table, the MTOANN presented the poorest prediction of the intended parameters. As for the SMANN and MVONN, although the SMA could train the more successfully, the performance of the MVO was more acceptable in the testing phase.

Furthermore, the used models showed different convergence behaviors. Back to Figure 5, it was shown that the EO, MTOA, WCA, and EFO approach the optimal response over the first 50 iterations, while SMA and MVO reached a similar level of the OF after several steps. Besides, the implementation time is another factor considered for this section. Optimizing the ANN using the EO, MTOA, SMA, MVO, EFO, and WCA took around 17506.7, 10344.6, 5270.5, 7274.8, 301.9, and 10888.3 seconds. Remarkably, the computer used for this research

Table 4 Accuracy comparison with previous studies

Study	Models*	Data							
		Training				Testing			
		L_H		L_C		L_H		L_{Cp}	
		MAE	RMSE	MAE	RMSE	MAE	RMSE	MAE	RMSE
Wu *et al*. (2020)	Backtracking Search Algorithm (BSA)	1.8556	2.5930	-	-	1.9083	2.6447	-	-
	Vortex Search Algorithm (VSA)	1.5794	2.1705	-	-	1.6193	2.2473	-	-
Zheng *et al*. (2020)	Moth-Flame Optimization (MFO)	-	-	1.9417	2.7479	-	-	1.900	2.6937
	Optics Inspired Optimization (OIO)	-	-	2.0542	2.9632	-	-	2.0793	2.9513
	Shuffled Complex Evolution (SCE)	-	-	1.8453	2.5468	-	-	1.8124	2.5943
Zhou *et al*. (2021a)	League Championship Algorithm (LCA)	-	-	2.0421	2.8720	-	-	2.0458	2.7751
	Cuckoo Optimization Algorithm (COA)	-	-	2.0339	2.9465	-	-	1.9525	2.8477
	Teaching–Learning-Based Optimization (TLBO)	-	-	1.8535	2.6263	-	-	1.8296	2.6297
Moayedi and Mosavi (2021b)	Biogeography-Based Optimization (BBO)	2.0846	2.5359	-	-	1.8284	2.4807	-	-
	Antlion Optimization Algorithm (ALO)	2.0992	2.6054	-	-	2.1865	2.7162	-	-
	Evolution Strategy (ES)	2.0848	2.7146	-	-	2.5072	3.0958	-	-
Guo *et al*. (2020)	Salp Swarm Optimization (SSA)	1.6737	2.4321	2.9087	2.0014	1.9178	2.7527	2.2424	3.1945
	Wind Driven Optimization (WDO)	1.7944	2.5896	2.1114	2.9942	1.9863	2.8312	2.1830	3.1471
Moayedi *et al*. (2020)	Ant Colony Optimization (ACO)	-	-	2.6333	3.5096	-	-	2.6011	3.3561
	Harris Hawks Optimization (HHO)	-	-	2.3972	3.3151	-	-	2.3265	3.1925
	Elephant Herding Optimization (EHO)	-	-	2.2652	3.1880	-	-	2.1284	3.0464
This study	WCA	1.1333	1.4509	1.6625	2.1764	1.1868	1.4866	1.6469	2.1767
	EO	1.3689	1.9188	1.7602	2.5221	1.5234	2.1296	1.8360	2.6459
	EFO	1.5268	2.1240	1.8229	2.5760	1.7284	2.3029	1.9353	2.6890

*All metaheuristic algorithms are combined with MLP neural network.

had a 64-bit operating system with Intel (R) Core (TM) i7-8565U CPU @ 1.80 GHz 1.99 GHz and 16 GB RAM. It indicates that the EFO (i.e., the third-accurate optimizer) provides the fastest technique for adjusting the biases and weights of the ANN.

3.4 Comparison with literature

Three outstanding models of this study are also compared to previously employed models in the earlier literature. Two accuracy criteria of MAE and RMSE are considered for this comparison because they were in common in all studies. Table 4 presents the results of this process. The considered models are backtracking search algorithm (BSA) and vortex search algorithm (VSA) used by Wu *et al*. (2020), moth-flame optimization (MFO), optics inspired optimization (OIO), shuffled complex evolution (SCE) used by Zheng *et al*. (2020), league championship algorithm (LCA), cuckoo optimization algorithm (COA), teaching–learning-based optimization (TLBO) used by Zhou *et al*. (2020b), biogeography-based optimization (BBO), antlion optimization algorithm (ALO), evolution strategy (ES) used by Moayedi and Mosavi (2021b), salp swarm optimization (SSA), wind driven optimization (WDO) used by Guo *et al*. (2020), and ant colony optimization (ACO), Harris hawks optimization (HHO), elephant herding optimization (EHO) used by Moayedi *et al*. (2020). As is seen, almost in all cases, the three elite models of the present study, i.e., WCA, EO, and EFO, outperformed previous models.

It indicates that these three algorithms are among the best optimizers for this purpose. Here, it should be also noted that the prediction of this study was for both the L_H and L_C. So, more complex ANNs have been optimized in this study.

Considering the values of MAE, we can say that the MAPEs of the above-mentioned algorithms are mostly expected to be greater than the those calculated in this study. It can be accordingly deduced that the relative errors of the WCA, EO, and EFO (which are MAPEs around 6, 7, and 8%) are in an acceptable level.

3.5 Formula extraction

Since the WCANN had a considerably higher accuracy for simultaneously predicting the L_H and L_C, this section presents a formula based on the WCA-optimized ANN. Back to Fig. 3, the ANN used in this work is composed of 8, 6, and 2 nodes in the first (i.e., input), second (i.e., hidden), and third (i.e., output) layer, respectively. Accordingly, there are 48 input-hidden weight factors, 12 hidden-output weight factors, 6 hidden biases, and 2 output biases to be optimized. Eqs. (12) and (13) yield the L_H and

L_C, respectively. These equations are elicited from the output nodes which are fed by the responses of the former layer (i.e., R_{Hid_1}, R_{Hid_2}, ... , R_{Hid_6}). Moreover, $f(x)$ represents the Tansig activation function (Eq. (20)).

$$L_{H_{WCANN}} = -0.602380 \times f(R_{Hid_1}) + 0.571768 \times f(R_{Hid_2}) - 0.028470 \times f(R_{Hid_3}) + 0.653163 \times f(R_{Hid_4}) - 0.873549 \times f(R_{Hid_5}) + 0.355007 \times f(R_{Hid_6}) - 0.417234 \quad (12)$$

$$L_{C_{WCANN}} = -0.172481 \times f(R_{Hid_1}) + 0.363220 \times f(R_{Hid_2}) - 0.609170 \times f(R_{Hid_3}) - 0.600067 \times f(R_{Hid_4}) - 0.419532 \times f(R_{Hid_5}) - 0.806426 \times f(R_{Hid_6}) - 0.758872 \quad (13)$$

$$R_{Hid_1} = 0.316828 \times C_R + 0.796085 \times S_A - 0.066714 \times S_W - 1.086300 \times S_R + 0.575320 \times H_T + 0.601761 \times O + 0.337141 \times S_G - 0.584946 \times DS_G - 1.751447 \quad (14)$$

$$R_{Hid_2} = 0.939006 \times C_R + 0.451372 \times S_A - 0.493652 \times S_W + 0.129236 \times S_R + 0.671360 \times H_T - 0.943172 \times O - 0.299024 \times S_G - 0.540360 \times DS_G - 1.050868 \quad (15)$$

$$R_{Hid_3} = -0.757236 \times C_R + 0.244966 \times S_A - 0.760031 \times S_W - 0.666510 \times S_R - 0.861318 \times H_T + 0.719287 \times O + 0.333703 \times S_G - 0.204129 \times DS_G + 0.350289 \quad (16)$$

$$R_{Hid_4} = 0.281771 \times C_R - 0.458422 \times S_A + 0.810135 \times S_W + 0.024695 \times S_R + 0.480164 \times H_T - 1.035814 \times O + 0.338409 \times S_G + 0.838512 \times DS_G + 0.350289 \quad (17)$$

$$R_{Hid_5} = 0.056005 \times C_R - 0.371050 \times S_A - 0.407042 \times S_W - 0.698628 \times S_R + 0.164256 \times H_T - 0.966020 \times O + 1.073893 \times S_G - 0.399458 \times DS_G + 1.050868 \quad (18)$$

$$R_{Hid_6} = 0.791290 \times C_R - 0.390577 \times S_A - 0.288624 \times S_W - 0.986351 \times S_R - 0.791514 \times H_T + 0.059304 \times O - 0.663635 \times S_G + 0.402816 \times DS_G + 1.751447 \quad (19)$$

$$f(x) = \frac{2}{1 + e^{-2x}} - 1 \quad (20)$$

3.6 Mechanism and solution

The methodology offered in this study is a smart evaluative model that facilitates the approximation of thermal load in residential buildings. It can provide fast, inexpensive, and optimized solutions for this problem without any need to laboratory experiments, heavy simulations, and field investigations. For instance, for upcoming building constructions, the heating and cooling loads can be predicted by having the geometry of the buildings so that the proper HVAC system be embedded.

Regarding the mechanism of the models, it has two major steps: 1) each input is first imported to an input neuron; then, the hidden neurons perform primary calculations and yield the results to two output neurons, and 2) these neurons then calculate and release the global outputs (i.e., the L_H and L_C) of the building.

The extracted formula can be reliably used where the calculations are regarded for identical data. For instance, the input parameters should not be different from the C_R, S_A, S_W, S_R, H_T, O, S_G, and DS_G. Also, a normalization is necessary as the neural network uses Tansig function whose outputs are between -1 and 1.

4. Conclusions

The heating load and cooling load are two significant factors in energy-efficiency analysis. This study, therefore, sought an efficient way of predicting these parameters. Water cycle algorithm, equilibrium optimizer, multi-tracker optimization algorithm, slime mould algorithm, multi-verse optimizer, and electromagnetic field optimization were the tested metaheuristic algorithms which assisted a neural network in discovering the relationship between the L_H and L_C with C_R, S_A, S_W, S_R, H_T, O, S_G, and DS_G. The first finding was that, due to the excellent agreement between the products of all hybrids with expected L_Hs and L_Cs (i.e., the R_Ps > 0.95 and 0.94, respectively), the incorporation of metaheuristic schemes with ANN can accurately predict these parameters. Next, it was derived that the solution suggested by the WCA can set up a more reliable ANN. This algorithm, however, took a longer time than MTOA, SMA, MVO, and EFO for minimizing the learning error. The EFO emerged as a very time-effective optimizer with the third-ranking of accuracy. Hence, this algorithm could be a proper substitute as well.

References

Abdel-Basset, M., Chang, V. and Mohamed, R. (2020), "A novel equilibrium optimization algorithm for multi-thresholding image segmentation problems", *Neural Comput. Applicat.*, 1-34. https://doi.org/10.1007/s00521-020-04820-y.

Abedinpourshotorban, H., Shamsuddin, S.M., Beheshti, Z. and Jawawi, D.N. (2016), "Electromagnetic field optimization: A physics-inspired metaheuristic optimization algorithm", *Swarm Evolut. Computat.*, **26**, 8-22. https://doi.org/10.1016/j.swevo.2015.07.002.

Ahmadi-Karvigh, S., Ghahramani, A., Becerik-Gerber, B. and Soibelman, L. (2018), "Real-time activity recognition for energy efficiency in buildings", *Appl. Energy*, **211**, 146-160. https://doi.org/10.1016/j.apenergy.2017.11.055.

Al-Shammari, E.T., Keivani, A., Shamshirband, S., Mostafaeipour, A., Yee, L., Petković, D. and Ch, S. (2016), "Prediction of heat load in district heating systems by Support Vector Machine with Firefly searching algorithm", *Energy*, **95**, 266-273. https://doi.org/10.1016/j.energy.2015.11.079.

Alam, A.G., Baek, C.I. and Han, H. (2016), "Prediction and analysis of building energy efficiency using artificial neural network and design of experiments", *Appl. Mech. Mater.*, 541-545. https://doi.org/10.4028/www.scientific.net/AMM.819.541.

Anderson, D. and McNeill, G. (1992), "Artificial neural networks technology", *Kaman Sciences Corp.*, **258**(6), 1-83.

Brabazon, A. and McGarraghy, S. (2020), "Slime mould foraging: an inspiration for algorithmic design", *Int. J. Innov. Comput. Applicat.*, **11**(1), 30-45. https://doi.org/10.1504/IJICA.2020.105316.

Bui, D.K., Nguyen, T.N., Ngo, T.D. and Nguyen-Xuan, H. (2020), "An artificial neural network (ANN) expert system enhanced with the electromagnetism-based firefly algorithm (EFA) for predicting the energy consumption in buildings", *Energy*, **190**, 116370. https://doi.org/10.1016/j.energy.2019.116370.

Çelik, E. and Gör, H. (2019), "Enhanced speed control of a DC servo system using PI+ DF controller tuned by stochastic fractal search technique", *J. Franklin Inst.*, **356**(3), 1333-1359. https://doi.org/10.1016/j.jfranklin.2018.11.020.

Çelik, E., Gör, H., Öztürk, N. and Kurt, E. (2017), "Application of artificial neural network to estimate power generation and efficiency of a new axial flux permanent magnet synchronous generator", *Int. J. Hydrogen Energy*, **42**(28), 17692-17699. https://doi.org/10.1016/j.ijhydene.2017.01.168.

Chou, J.S. and Bui, D.K. (2014), "Modeling heating and cooling loads by artificial intelligence for energy-efficient building design", *Energy Build.*, **82**, 437-446. https://doi.org/10.1016/j.enbuild.2014.07.036.

Chou, J.S. and Ngo, N.T. (2016), "Time series analytics using sliding window metaheuristic optimization-based machine learning system for identifying building energy consumption patterns", *Appl. Energy*, **177**, 751-770. https://doi.org/10.1016/j.apenergy.2016.05.074.

Chung, W., Hui, Y.V. and Lam, Y.M. (2006), "Benchmarking the energy efficiency of commercial buildings", *Appl. Energy*, **83**(1), 1-14. https://doi.org/10.1016/j.apenergy.2004.11.003.

Das, M., Singh, M.A.K. and Biswas, A. (2019), "Techno-economic optimization of an off-grid hybrid renewable energy system using metaheuristic optimization approaches–case of a radio transmitter station in India", *Energy Convers. Manage.*, **185**, 339-352. https://doi.org/10.1016/j.enconman.2019.01.107

Dunlop, T. (2019), "Mind the gap: A social sciences review of energy efficiency", *Energy Res. Soc. Sci.*, **56**, 101216. https://doi.org/10.1016/j.erss.2019.05.026.

Ekici, B.B. and Aksoy, U.T. (2011), "Prediction of building energy needs in early stage of design by using ANFIS", *Expert Syst. Applicat.*, **38**(5), 5352-5358. https://doi.org/10.1016/j.eswa.2010.10.021.

EMSD (2019), Energy end-use data.

Eskandar, H., Sadollah, A., Bahreininejad, A. and Hamdi, M. (2012), "Water cycle algorithm–A novel metaheuristic optimization method for solving constrained engineering optimization problems", *Comput. Struct.*, **110**, 151-166. https://doi.org/10.1016/j.compstruc.2012.07.010.

Faramarzi, A., Heidarinejad, M., Stephens, B. and Mirjalili, S. (2020), "Equilibrium optimizer: A novel optimization algorithm", *Knowl.-Bas. Syst.*, **191**, 105190. https://doi.org/10.1016/j.knosys.2019.105190.

Fathy, A. and Rezk, H. (2018), "Multi-verse optimizer for identifying the optimal parameters of PEMFC model", *Energy*, **143**, 634-644. https://doi.org/10.1016/j.energy.2017.11.014.

Feng, Y., Zhang, B., Liu, Y., Niu, Z., Dai, B., Fan, Y. and Chen, X. (2021), "A 200–225-GHz manifold-coupled multiplexer utilizing metal waveguides", *IEEE Trans. Microw. Theory Techniq.*, **69**(12), 5327-5333. https://doi.org/10.1109/TMTT.2021.3119316.

Foong, L.K., Moayedi, H. and Lyu, Z. (2020), "Computational modification of neural systems using a novel stochastic search scheme, namely evaporation rate-based water cycle algorithm: an application in geotechnical issues", *Eng. Comput.*, **37**(4), 3347-3358. https://doi.org/10.1007/s00366-020-01000-3.

Ghiasi, M.M., Arabloo, M., Mohammadi, A.H. and Barghi, T. (2016), "Application of ANFIS soft computing technique in modeling the CO_2 capture with MEA, DEA, and TEA aqueous solutions", *Int. J. Greenhouse Gas Control*, **49**, 47-54. https://doi.org/10.1016/j.ijggc.2016.02.015.

Gor, H. and Kurt, E. (2016), "Waveform characteristics and losses of a new double sided axial and radial flux generator", *Int. J. Hydrogen Energy*, **41**(29), 12512-12524. https://doi.org/10.1016/j.ijhydene.2015.12.172.

Guo, Z., Moayedi, H., Foong, L.K. and Bahiraei, M. (2020), "Optimal modification of heating, ventilation, and air conditioning system performances in residential buildings using the integration of metaheuristic optimization and neural computing", *Energy Build.*, **214**, 109866. https://doi.org/10.1016/j.enbuild.2020.109866.

Hakim, S.J.S. and Razak, H.A. (2014), "Modal parameters based structural damage detection using artificial neural networks-a review", *Smart Struct. Syst.*, **14**(2), 159-189. https://doi.org/10.12989/sss.2014.14.2.159.

Hecht-Nielsen, R. (1992), *Neural Networks for Perception*, Elsevier, 65-93. https://doi.org/10.1016/B978-0-12-741252-8.50010-8.

Homod, R.Z., Togun, H., Abd, H.J. and Sahari, K.S. (2020), "A novel hybrid modelling structure fabricated by using Takagi-Sugeno fuzzy to forecast HVAC systems energy demand in real-time for Basra city", *Sustain. Cities Soc.*, **56**, 102091. https://doi.org/10.1016/j.scs.2020.102091.

Hornik, K., Stinchcombe, M. and White, H. (1989), "Multilayer feedforward networks are universal approximators", *Neur. Network.*, **2**(5), 359-366. https://doi.org/10.1016/0893-6080(89)90020-8.

Huang, Y., Niu, J.L. and Chung, T.M. (2014), "Comprehensive analysis on thermal and daylighting performance of glazing and shading designs on office building envelope in cooling-dominant climates", *Appl. Energy*, **134**, 215-228. https://doi.org/10.1016/j.apenergy.2014.07.100.

Ikeda, S. and Ooka, R. (2015), "Metaheuristic optimization methods for a comprehensive operating schedule of battery, thermal energy storage, and heat source in a building energy system", *Appl. Energy*, **151**, 192-205. https://doi.org/10.1016/j.apenergy.2015.04.029.

International Energy Agency (IEA) (2019), *Key world energy statistics*, OECD, Paris, France.

Jangir, P., Parmar, S.A., Trivedi, I.N. and Bhesdadiya, R.H. (2017), "A novel hybrid particle swarm optimizer with multi verse optimizer for global numerical optimization and optimal reactive power dispatch problem", *Eng. Sci. Technol.*, **20**(2), 570-586. https://doi.org/10.1016/j.jestch.2016.10.007.

Khosravi, H., Zakeri, E., Xie, W.F. and Ahmadi, B. (2020),

"Adaptive multi-tracker optimization algorithm for global optimization problems: emphasis on applications in chemical engineering", *Eng. Comput.*, 1-28. https://doi.org/10.1007/s00366-020-01101-z.

Koschwitz, D., Frisch, J. and Van Treeck, C. (2018), "Data-driven heating and cooling load predictions for non-residential buildings based on support vector machine regression and NARX Recurrent Neural Network: A comparative study on district scale", *Energy*, **165**, 134-142. https://doi.org/10.1016/j.energy.2018.09.068.

Kumar, S., Pal, S.K. and Singh, R.P. (2018), "A novel method based on extreme learning machine to predict heating and cooling load through design and structural attributes", *Energy Build.*, **176**, 275-286. https://doi.org/10.1016/j.enbuild.2018.06.056.

Kurt, E. and Gör, H. (2014), "Electromagnetic design of a new axial flux generator", *Proceedings of the 2014 6th International Conference on Electronics, Computers and Artificial Intelligence (ECAI)*, 39-42. https://doi.org/10.1109/ECAI.2014.7090195.

Le, L.T., Nguyen, H., Dou, J. and Zhou, J. (2019a), "A comparative study of PSO-ANN, GA-ANN, ICA-ANN, and ABC-ANN in estimating the heating load of buildings' energy efficiency for smart city planning", *Appl. Sci.*, **9**(13), 2630. https://doi.org/10.3390/app9132630.

Le, L.T., Nguyen, H., Zhou, J., Dou, J. and Moayedi, H. (2019b), "Estimating the heating load of buildings for smart city planning using a novel artificial intelligence technique PSO-XGBoost", *Appl. Sci.*, **9**(13), 2714. https://doi.org/10.3390/app9132714.

Li, Z.J. and Zhang, K. (2008), "Comparison of three GIS-based hydrological models", *J. Hydrol. Eng.*, **13**(5), 364-370. https://doi.org/10.1061/(ASCE)1084-0699(2008)13:5(364).

Li, Q., Meng, Q., Cai, J., Yoshino, H. and Mochida, A. (2009a), "Applying support vector machine to predict hourly cooling load in the building", *Appl. Energy*, **86**(10), 2249-2256. https://doi.org/10.1016/j.apenergy.2008.11.035.

Li, Q., Meng, Q., Cai, J., Yoshino, H. and Mochida, A. (2009b), "Predicting hourly cooling load in the building: A comparison of support vector machine and different artificial neural networks", *Energy Convers. Manage.*, **50**(1), 90-96. https://doi.org/10.1016/j.enconman.2008.08.033.

Li, S., Chen, H., Wang, M., Heidari, A.A. and Mirjalili, S. (2020), "Slime mould algorithm: A new method for stochastic optimization", *Future Gener. Comput. Syst.*, **111**, 300-323. https://doi.org/10.1016/j.future.2020.03.055.

Li, A., Xiao, F., Zhang, C. and Fan, C. (2021a), "Attention-based interpretable neural network for building cooling load prediction", *Appl. Energy*, **299**, 117238. https://doi.org/10.1016/j.apenergy.2021.117238.

Li, X., Gui, D., Zhao, Z., Li, X., Wu, X., Hua, Y., Guo, P. and Zhong, H. (2021b), "Operation optimization of electrical-heating integrated energy system based on concentrating solar power plant hybridized with combined heat and power plant", *J. Cleaner Product.*, **289**, 125712. https://doi.org/10.1016/j.jclepro.2020.125712.

Liang, S., Foong, L.K. and Lyu, Z. (2020), "Determination of the friction capacity of driven piles using three sophisticated search schemes", *Eng. Comput.*, 1-13. https://doi.org/10.1007/s00366-020-01118-4.

Luo, Q., Wen, C., Qiao, S. and Zhou, Y. (2016), "Dual-system water cycle algorithm for constrained engineering optimization problems", *International Conference on Intelligent Computing*, pp. 730-741. https://doi.org/10.1007/978-3-319-42291-6_73.

Macas, M., Moretti, F., Fonti, A., Giantomassi, A., Comodi, G., Annunziato, M., Pizzuti, S. and Capra, A. (2016), "The role of data sample size and dimensionality in neural network based forecasting of building heating related variables", *Energy Build.*, **111**, 299-310. https://doi.org/10.1016/j.enbuild.2015.11.056.

Martin, G.L., Monfet, D., Nouanegue, H.F., Lavigne, K. and Sansregret, S. (2019), "Energy calibration of HVAC sub-system model using sensitivity analysis and meta-heuristic optimization", *Energy Build.*, **202**, 109382. https://doi.org/10.1016/j.enbuild.2019.109382.

McQuiston, F.C., Parker, J.D. and Spitler, J.D. (1982), *Heating, Ventilating, and Air Conditioning: Analysis and Design*, John Wiley & Sons.

Mehrabi, M., Pradhan, B., Moayedi, H. and Alamri, A. (2020), "Optimizing an adaptive neuro-fuzzy inference system for spatial prediction of landslide susceptibility using four state-of-the-art metaheuristic techniques", *Sensors*, **20**(6), 1723. https://doi.org/10.3390/s20061723.

Mirjalili, S., Mirjalili, S.M. and Hatamlou, A. (2016), "Multi-verse optimizer: a nature-inspired algorithm for global optimization", *Neural Comput. Applicat.*, **27**(2), 495-513. https://doi.org/10.1007/s00521-015-1870-7.

Moayedi, H. and Mosavi, A. (2021a), "Suggesting a stochastic fractal search paradigm in combination with artificial neural network for early prediction of cooling load in residential buildings", *Energies*, **14**(6), 1649. https://doi.org/10.3390/en14061649.

Moayedi, H. and Mosavi, A. (2021b), "Synthesizing multi-layer perceptron network with ant lion biogeography-based dragonfly algorithm evolutionary strategy invasive weed and league champion optimization hybrid algorithms in predicting heating load in residential buildings", *Sustainability*, **13**(6), 3198. https://doi.org/10.3390/su13063198.

Moayedi, H., Mehrabi, M., Mosallanezhad, M., Rashid, A.S.A. and Pradhan, B. (2019), "Modification of landslide susceptibility mapping using optimized PSO-ANN technique", *Eng. Comput.*, **35**(3), 967-984. https://doi.org/10.1007/s00366-018-0644-0.

Moayedi, H., Mu'azu, M.A. and Foong, L.K. (2020), "Novel swarm-based approach for predicting the cooling load of residential buildings based on social behavior of elephant herds", *Energy Build.*, **206**, 109579. https://doi.org/10.1016/j.enbuild.2019.109579.

Moradzadeh, A., Mansour-Saatloo, A., Mohammadi-Ivatloo, B. and Anvari-Moghaddam, A. (2020), "Performance evaluation of two machine learning techniques in heating and cooling loads forecasting of residential buildings", *Appl. Sci.*, **10**(11), 3829. https://doi.org/10.3390/app10113829.

Nasir, M., Sadollah, A., Choi, Y.H. and Kim, J.H. (2020), "A comprehensive review on water cycle algorithm and its applications", *Neural Comput. Applicat.*, **32**(23), 17433-17488. https://doi.org/10.1007/s00521-020-05112-1.

Nehdi, M. and Greenough, T. (2007), "Modeling shear capacity of RC slender beams without stirrups using genetic algorithms", *Smart Struct. Syst., Int. J.*, **3**(1), 51-68. https://doi.org/10.12989/sss.2007.3.1.051.

Nguyen, H., Mehrabi, M., Kalantar, B., Moayedi, H. and Abdullahi, M.A.M. (2019), "Potential of hybrid evolutionary approaches for assessment of geo-hazard landslide susceptibility mapping", *Geomat. Natural Hazards Risk*, **10**(1), 1667-1693. https://doi.org/10.1080/19475705.2019.1607782.

Nilashi, M., Dalvi-Esfahani, M., Ibrahim, O., Bagherifard, K., Mardani, A. and Zakuan, N. (2017), "A soft computing method for the prediction of energy performance of residential buildings", *Measurement*, **109**, 268-280. https://doi.org/10.1016/j.measurement.2017.05.048.

Ouarghi, R. and Krarti, M. (2006), "Building Shape Optimization Using Neural Network and Genetic Algorithm Approach", *Ashrae Transact.*, **112**(1).

Yıldız, A.R., Özkaya, H., Yıldız, M., Bureerat, S., Yıldız, B.S. and

Sait, S.M. (2020), "The equilibrium optimization algorithm and the response surface-based metamodel for optimal structural design of vehicle components", *Mater. Test.*, **62**(5), 492-496.

Palm, J. and Thollander, P. (2010), "An interdisciplinary perspective on industrial energy efficiency", *Appl. Energy*, **87**(10), 3255-3261. https://doi.org/10.1016/j.apenergy.2010.04.019.

Pinkus, A. (1999), "Approximation theory of the MLP model in neural networks", *Acta Numerica*, **8**, 143-195. https://doi.org/10.1017/S0962492900002919.

Qiao, W., Moayedi, H. and Foong, L.K. (2020), "Nature-inspired hybrid techniques of IWO, DA, ES, GA, and ICA, validated through a k-fold validation process predicting monthly natural gas consumption", *Energy Build.*, 110023. https://doi.org/10.1016/j.enbuild.2020.110023.

Reddy, A.V.R. and Kumar, M.S. (2019), "A Comparative Analysis of Regression Algorithms for Energy Estimation in Residential Buildings", *International Conference on Intelligent Computing and Communication Technologies*, 300-311. https://doi.org/10.1007/978-981-13-8461-5_33.

Roberts, A. and Marsh, A. (2001), ECOTECT: Environmental Prediction in Architectural Education.

Roy, S.S., Roy, R. and Balas, V.E. (2018), "Estimating heating load in buildings using multivariate adaptive regression splines, extreme learning machine, a hybrid model of MARS and ELM", *Renew. Sustain. Energy Rev.*, **82**, 4256-4268. https://doi.org/10.1016/j.rser.2017.05.249.

Schwalm, C.R., Huntinzger, D.N., Michalak, A.M., Fisher, J.B., Kimball, J.S., Mueller, B., Zhang, K. and Zhang, Y. (2013), "Sensitivity of inferred climate model skill to evaluation decisions: a case study using CMIP5 evapotranspiration", *Environ. Res. Lett.*, **8**(2), 024028. https://doi.org/10.1088/1748-9326/8/2/024028.

Seyedashraf, O., Mehrabi, M. and Akhtari, A.A. (2018), "Novel approach for dam break flow modeling using computational intelligence", *J. Hydrol.*, **559**, 1028-1038. https://doi.org/10.1016/j.jhydrol.2018.03.001.

Seyedzadeh, S., Rahimian, F.P., Rastogi, P. and Glesk, I. (2019), "Tuning machine learning models for prediction of building energy loads", *Sustain. Cities Soc.*, **47**, 101484. https://doi.org/10.1016/j.scs.2019.101484.

Seyedzadeh, S., Rahimian, F.P., Oliver, S., Glesk, I. and Kumar, B. (2020), "Data driven model improved by multi-objective optimisation for prediction of building energy loads", *Automat. Constr.*, **116**, 103188. https://doi.org/10.1016/j.autcon.2020.103188.

Shariati, M., Mafipour, M.S., Mehrabi, P., Ahmadi, M., Wakil, K., Trung, N.T. and Toghroli, A. (2020), "Prediction of concrete strength in presence of furnace slag and fly ash using Hybrid ANN-GA (Artificial Neural Network-Genetic Algorithm)", *Smart Struct. Syst.*, **25**(2), 183-195. https://doi.org/10.12989/sss.2020.25.2.183.

Silva, B.N., Khan, M. and Han, K. (2018), "Towards sustainable smart cities: A review of trends, architectures, components, and open challenges in smart cities", *Sustain. Cities Soc.*, **38**, 697-713. https://doi.org/10.1016/j.scs.2018.01.053.

Song, S., Jia, H. and Ma, J. (2019), "A chaotic electromagnetic field optimization algorithm based on fuzzy entropy for multilevel thresholding color image segmentation", *Entropy*, **21**(4), 398. https://doi.org/10.3390/e21040398.

Talebi, B. and Dehkordi, M.N. (2018), "Sensitive association rules hiding using electromagnetic field optimization algorithm", *Expert Syst. Applicat.*, **114**, 155-172. https://doi.org/10.1016/j.eswa.2018.07.031.

Tran, D.H., Luong, D.L. and Chou, J.S. (2020), "Nature-inspired metaheuristic ensemble model for forecasting energy consumption in residential buildings", *Energy*, **191**, 116552. https://doi.org/10.1016/j.energy.2019.116552.

Tsanas, A. and Xifara, A. (2012), "Accurate quantitative estimation of energy performance of residential buildings using statistical machine learning tools", *Energy Build.*, **49**, 560-567. https://doi.org/10.1016/j.enbuild.2012.03.003.

Vine, E. (2003), "Opportunitites for promoting energy efficiency in buildings as an air quality compliance approach", *Energy*, **28**(4), 319-341. https://doi.org/10.1016/S0360-5442(02)00112-3.

Wu, D., Foong, L.K. and Lyu, Z. (2020), "Two neural-metaheuristic techniques based on vortex search and backtracking search algorithms for predicting the heating load of residential buildings", *Eng. Comput.*, 1-14. https://doi.org/10.1007/s00366-020-01074-z.

Xu, J., Wu, Z., Chen, H., Shao, L., Zhou, X. and Wang, S. (2021), "Study on strength behavior of basalt fiber-reinforced loess by digital image technology (DIT) and scanning electron microscope (SEM)", *Arab. J. Sci. Eng.*, **46**(11), 11319-11338. https://doi.org/10.1007/s13369-021-05787-1.

Yaïci, W. and Entchev, E. (2016), "Adaptive neuro-fuzzy inference system modelling for performance prediction of solar thermal energy system", *Renew. Energy*, **86**, 302-315. https://doi.org/10.1016/j.renene.2015.08.028.

Ye, X., Moayedi, H., Khari, M. and Foong, L.K. (2020), "Metaheuristic-hybridized multilayer perceptron in slope stability analysis", *Smart Struct. Syst.*, **26**(3), 263-275. https://doi.org/10.12989/sss.2020.26.3.263.

Zakeri, E., Moezi, S.A., Bazargan-Lari, Y. and Zare, A. (2017), "Multi-tracker optimization algorithm: a general algorithm for solving engineering optimization problems", *Iran. J. Sci. Technol. Trans. Mech. Eng.*, **41**(4), 315-341. https://doi.org/10.1007/s40997-016-0066-9.

Zeynali, S., Rostami, N., Ahmadian, A. and Elkamel, A. (2020), "Two-stage stochastic home energy management strategy considering electric vehicle and battery energy storage system: An ANN-based scenario generation methodology", *Sustain. Energy Technol. Assessm.*, **39**, 100722. https://doi.org/10.1016/j.seta.2020.100722.

Zhang, K., Chao, L.J., Wang, Q.Q., Huang, Y.C., Liu, R.H., Hong, Y., Tu, Y., Qu, W. and Ye, J.Y. (2019), "Using multi-satellite microwave remote sensing observations for retrieval of daily surface soil moisture across China", *Water Sci. Eng.*, **12**(2), 85-97. https://doi.org/10.1016/j.wse.2019.06.001.

Zhang, Y., Pan, G., Chen, B., Han, J., Zhao, Y. and Zhang, C. (2020), "Short-term wind speed prediction model based on GA-ANN improved by VMD", *Renew. Energy*, **156**, 1373-1388. https://doi.org/10.1016/j.renene.2019.12.047.

Zhang, C., Ali, A. and Sun, L. (2021), "Investigation on low-cost friction-based isolation systems for masonry building structures: Experimental and numerical studies", *Eng. Struct.*, **243**, 112645. https://doi.org/10.1016/j.engstruct.2021.112645.

Zhao, J. and Liu, X. (2018), "A hybrid method of dynamic cooling and heating load forecasting for office buildings based on artificial intelligence and regression analysis", *Energy Build.*, **174**, 293-308. https://doi.org/10.1016/j.enbuild.2018.06.050.

Zheng, S., Lyu, Z. and Foong, L.K. (2020), "Early prediction of cooling load in energy-efficient buildings through novel optimizer of shuffled complex evolution", *Eng. Comput.*, 1-15. https://doi.org/10.1007/s00366-020-01140-6.

Zhou, G., Moayedi, H., Bahiraei, M. and Lyu, Z. (2020a), "Employing artificial bee colony and particle swarm techniques for optimizing a neural network in prediction of heating and cooling loads of residential buildings", *J. Cleaner Product.*, **254**, 120082. https://doi.org/10.1016/j.jclepro.2020.120082.

Zhou, G., Moayedi, H. and Foong, L.K. (2020b), "Teaching–learning-based metaheuristic scheme for modifying neural computing in appraising energy performance of building", *Eng. Comput.*, **37**(4), 3037-3048. https://doi.org/10.1007/s00366-020-00981-5.

Zhou, G., Moayedi, H. and Foong, L.K. (2021a), "Teaching–learning-based metaheuristic scheme for modifying neural computing in appraising energy performance of building", *Eng. Comput.*, **37**(4), 3037-3048. https://doi.org/10.1007/s00366-020-00981-5.

Zhou, W., Liu, J., Lei, J., Yu, L. and Hwang, J.N. (2021b), "GMNet: graded-feature multilabel-learning network for RGB-thermal urban scene semantic segmentation", *IEEE Transact. Image Process.*, **30**, 7790-7802. https://doi.org/10.1109/TIP.2021.3109518.

CC